

A Review on Energy Optimization in QCA Platform

Suparba Tapna

Department of Electronics & Communication
Engineering, Brainware University,
Barasat, West Bengal, India

Debarka Mukhopadhyay

Department of Computer Science & Engineering, Faculty of
Engineering, CHRIST (Deemed to be University),
Bangalore, Karnataka, India

Kisalaya Chakrabarti

Department of Electronics & Communication Engineering, Haldia Institute of Technology,
Haldia, West Bengal, India

Abstract:- Another nanotechnology model called QCA, or "Quantum Dot-Cellular Automata," provides an alternative solution for CMOS, which has a lot of hardware limitations and a lot of real cutoff points. Data is passed based on electron charge and by their shared electrostatic repugnance in QCA, a semiconductor-free innovation. The device thickness, exchanging speed timing, and force utilisation of QCA are remarkably higher. QCA circuits may play a big role in cryptographic applications. Using a QCA-based rationale circuit, encryption and decryption operations are carried out. The research paper illustrates a fundamental QCA cypher text creation method that could be helpful for secure QCA-based nano-communication. Finding a practical so-lution for secured authentication is the focus of secured encryption. Using the QCA Designer-2.0.3 tool, the results are executed and tested.

Keywords:- Cipher · Quantum Dot Cellular Automata(QCA) · Clocking Scheme · Mux and Demux with Parity · Majority Gate · PRBS · Schrodinger Equation for Quantum Enhancement · Security for Quantum Level · N Value for Quantized States.

I. INTRODUCTION

QCA is basically the nanotechnology, which could be utilized with the semi-conductor-based CMOS system as an elective response. CMOS circuit have issue in their planning as its various segments relies upon one another and furthermore have numerous actual cutoff points [1],[5]. Thus, in CMOS circuit future adaptability is the most concerning issue in light of the fact that no of cells at nanoscale implanted in a solitary chip will increment along with circuit synchronization intricacy will expand much more and limited to few actual wonders. By utilizing QCA, this issue can be tackled as QCA is semiconductor having high thickness, higher timing recurrence along with low force utilization [3],[4].

In time, it is necessary to reduce the size to design a coordinated circuit, for example by increasing the circuit thickness. So we have to switch from semiconductor to semiconductor and QCA provides the opportunity. Electron charges present in the Quantum Dots are transmitted by QCA data irrespec-tive of electrical energy (beat), as in CMOS

[8],[9] circuits. In cryptography assumes significant part for addressing the real information into an encoded (non-discernible) from unsecured to secured transformation to get authentic information[12],[13]. This specific article depicts a straightforward method to produce cipher text utilizing QCA. The simulation of the proposed imple-mentation is utilizing QCA Designer-2.0.3[10],[11]. The organization of entire manuscript represent for section 2 is overview of QCA ,section 3 briefly de-cribe about QCA clocking,section 4 for secure nanocommunication utilizing in QCA.After section 4 we are discussing about PRBS in fifth section and reducing the bit error rate in channel coding in section 6 & results and dis-cussion is represented in section7.The last section is concluding about this research work.

II. QCA OVERVIEW

The overall implication is assumed from Quantum Dot Cellular Automata(QCA) perspective. With such a nanotechnology phenomenon are correlated to con-struct in the finding of this paradigm which is very suitable for the proposed approach and also indicated in this research work in a true manner.

➤ QCA Cell

The essentials of four dots of the QCA [4],[16], which can bind an electron within, are presented in Fig. 1(a). Each speck has a burrowing wire that can burrow through each of the four dots, connecting them to each other. Another 2 free electrons were applied to the cell of QCA and as the electrons repel each other, they were placed within QCA in antipodal conditions. There can be two distinct designs of QCA cell, named QCA cell polarization and defined by P, contingent on this electron situation. As demonstrated in fig1 (b) as well as fig1(c).

$P=+1$ along with $P=-1$ demonstrates parallel binary logic such as '1' as well as '0' separately whereas $P=0$ indicates null cell such that contains no data. [17],[18]

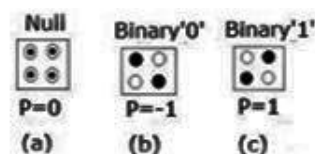


Fig 1 Cell Polarization of Different QCA

➤ Overview of Majority Gate

Majority gate for three i/p is essential rationale entryways utilized in a QCA that monetizes according to the majority gate of the data source[21],[22]. Sup-pose A, B, C be three contributions to majority gate, at that point rationale work for dominant part entryway may be composed as

$$F(A, B, C) = AB + BC + CA \quad (I)$$

If we fixed its contribution estimation to logic values ‘0’ as well as ‘1’, at that point rationale AND- gate or potentially entryway may be formulated individually [17],[20] composed as:

$$F(A, B, 0) = A.B \quad (II)$$

$$F(A, B, 1) = A + B \quad (III)$$

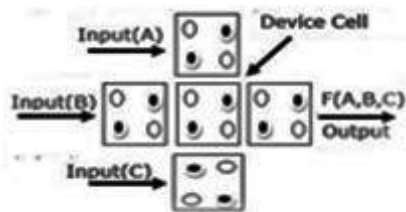


Fig 2 Realization of Majority Gate for Predicted o/p[8]

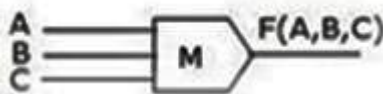


Fig 3 Realization of Majority Gate for Predicted o/p[8]

Table 1 Majority Gate Truth Table

A	B	C	F(A, B, C)
0	0	0	0
0	0	1	0
0	1	0	0
0	1	1	1
1	1	0	1
1	0	1	1
1	1	0	1
1	1	1	1

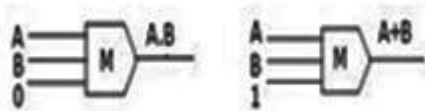


Fig 4 AND- Gate and OR- Gate in QCA[8]

➤ Wire Logic in QCA

QCA wire can be formed near setting about QCA cell continuously, whereas data is conveying by electrostatic communication among cells of QCA. These wire assists with conveying data inside a QCA circuit. fig.4 (a) and (b) shows the two unique sorts of QCA wire [18] [21]. The polarization in 90° QCA wire stays similar in whole QCA exhibit whereas the polarization in 45° QCA wire substitutes in each continuous cell in cluster[25],[26].

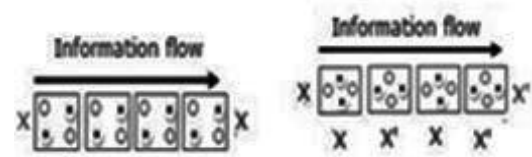


Fig 5 90° wire and 45° wire in QCA[8]

➤ Inverter Circuit in QCA

As given in Fig.5, QCA inverter may be shaped when at 45°point QCA cells sets (corners contacting) as demonstrated in [20],[21]. Because of electrostatic repugnance among cells, ‘0’ and ‘1’ will be the set logic values that can be changed over to ‘1’ as well as ‘0’ separately.

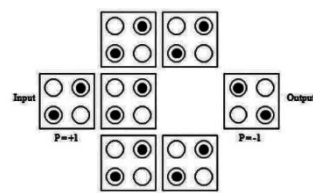


Fig 6 QCA inverters[8]

III. QCA CLOCKING

QCA timing has total 4 stages slacking by π/2 [10],[19] as demonstrated in Fig.6 that makes another way to plan nano-circuit not the same as CMOS circuits [24].

Switch stage—the boundary among QCA cell dabs is increased. The specks are affected through its adjoining electron where electron begins burrowing among dabs. Hence, QCA cell gets energized. Hold stage— Cell’s hindrance stays high where electron can’t burrow among dots as well as cell keeps up its present statuses (fixed polarization).

Release stage—hindrance among spots are brought down, electron may burrow through specks as well as QCA cell become un-enraptured.

Relax stage—hindrance stay at brought down along with cell stays in un-captivated state.

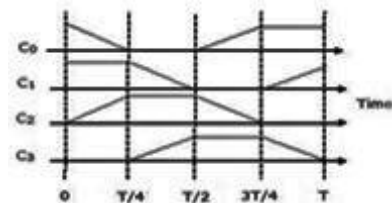


Fig 7 Four Phase Clocking [2]

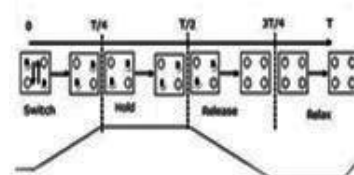


Fig 8 QCA Operation During One Clock Phase [2]

IV. LITERATURE SURVEY BASED ON QUANTUM CRYPTOGRAPHY TECHNOLOGY

Data security is a major concern while transmitting data, as the authors Bikash Debnath, Jadav Chandra Das, and Debashis De describe in "Cryptographic models of nanocommunicaton network employing quantum dot cellular au-tomata" [32]. The encoder and decoder, respectively, are the devices that carry out the encoding and unwinding processes. The complexity of the circuitry and power dispersion at the nanoscale are the main obstacles to the development of such devices. The solution to this problem is to use the advantages of re-versible reasoning using a Quantum Dot Cellular Automata (QCA) device as a promising paradigm for an alternative to the traditional semiconductor-based device. QCA has excellent protection against side-channel attacks, espe-cially those originating from power examination attacks. Each of those QCA components influences the analysts' decision to look into a few QCA-based cryptographic models of nanocommunication for safe data transmission. Here, the existing QCA-based cryptographic engineering circuits are examined and studied in terms of their circuit complexity, device area, and processing speeds. Each of those modern designs has been thoroughly demonstrated in terms of how it functions. Moreover, the introduction of reversible logic into QCA cryp-tography design is also examined. The designs are examined in terms of the reasoning behind the plan. Finally, with relation to cryptographic models for upcoming safe information transmission operations, the key essential issues of interest are identified and addressed. The authors of "Cryptography in Quan-tum Cellular Automata," Mohammad Amin Amiri, Sattar Mirzakuchaki, and Mojdeh Mahdavi [33] discuss how in recent years, the semiconductor industry has worked to increase the speed, power efficiency, and joining of coordinated circuits by shrinking semiconductor element sizes. In any event, it seems that some difficulties, such power utilisation, can't be ignored even if the semicon-ductor estimations are reduced. QCA, which was initially introduced by Lent et al. (Lent et al., 1993)cite, targets a nano-level breakthrough that is currently in the making. One technique for reducing the power consumption of these cir-cuits is to implement rationale circuits using the QCA invention, which also increases the clock recurrence of these circuits to terahertz frequencies and reduces their size to the nanoscale (Lent et al., 1993) [25]; Tougaw and Lent, 1994" "[26]" Quantum dots in QCA cells allow the position of the electrons to determine the double degrees of 0 and 1. The most obvious component of QCA that goes against the conventional logic that consistent states are stored by voltage levels is this. Cutting edge Encryption Standard finalist rival was the serpent block figure (AES). This 32-round cryptographic calculation uses a 256-cycle key size and a 128-bit block size. The final stage FP, 32 rounds, and an underlying change IP make up this cryptographic calculation. Key blending exercises, pass-through S-boxes, and a straight change are all included in each round. In the final cycle, an additional key blending operation takes the place of the straight change (Anderson et al., 1998) [31]. In their paper

titled "DE-SIGN AND ANALYSIS OF QCA CRYPTOGRAPHIC CIRCUITS," Mansi Rana and Mr. Ajay Dagar mention in citation [35] that The two main components of this model's all-out QCA circuits restriction are switch power and spillage strength. The power misfortune is set as a spillage during clock oscil-lations from low to high or high to low and the influence misfortune is set as an exchanging influence during the exchanging time period. More recently, re-search has encouraged more proficient designing of various QCA architectures. The design of the memory cell, a crucial component in QCA devices, has also received a lot of attention. For instance, there are many superior plans for QCA devices rationale circuits using choose or gates switch entryways and other al-ternative QCA wiring approaches. While the processes for planning each of these circuits independently have been set forth, the overall plan demands, the ring-based QCA methods are a pioneering approach for planning fantastic with the aggressive purpose of developing conventional CMOS based Smash (SRAM). Watchwords: CMOS, Slam, and QCA Apparatuses (SRAM) The authors of the article "Hardware Security based Quantum Dot Cellular Au-tomata Circuit Design" - Review and Outlook, M. Amutha and K.R. Kavitha, [34], primarily focus on the fact that in recent times, CMOS innovation has assumed a crucial role in VLSI-based IC innovation, which is a combination of logical models. The activities performed by the chip have improved signifi-cantly over time. The semiconductor has to be contracted in order to increase chips. The scaling system in CMOS innovation has led to significant challenges in force utilisation, actual aspects, and current spillages. Quantum Cell Au-tomata (QCA), among the possible configurations, is regarded as the most promising development due to its potential uses in computing schemes with alluring features like low power consumption, quick activity, and high device thickness. For various circuits, such as adders, multipliers, memories, cryp-tographic processors, and nano-specialized devices, the QCA provides better solutions. Actual equipment attacks have more severe side effects, and recovery is difficult. The focus of the article will be equipment security. Hyun-II Kim and Jun-Cheol Jeon's research paper "Quantum LFSR Structure for Random Number Generation Using QCA Multilayered Shift Register for Cryptographic Purposes" [36] as an example. A direct criticism shift register can be used to plan a Regular number generator (RNG), a cryptographic invention that is important in security and sensor organisations (LFSR). CMOS currently han-dles this cryptographic modification. It was made by reducing the size of the door and raising the amount of reconciliation, but due to the uniqueness of quantum burrowing, it has reached the breaking point of joining. One of the quantum circuit design advancements to replace this is the quantum-spot cell automata (QCA), which has superior performance to CMOS in most execution zones, including space, speed, and power. The majority of the LFSRs in the current QCA are designed as shift registers (SR), and the majority of the SR circuits offered are planar. As a result, when a plane convergence is performed, the phone region is large and the sign is shaky. Thus, we propose a sophisti-cated 2-to-1 QCA multiplexer and a D-latch in this work. We also make blocks in light of the D-lock and connect these blocks to create SR. Similar to how the LFSR structure is planned,

we also suggest an LFSR that is capable of double edge setting off. The proposed structures have superior performance compared to many existing circuits since they were designed with a very rigorous plan strategy to reduce area and idleness using cell connection. The cost and energy distribution of the suggested buildings are calculated through re-production using QCA Designer and QCA Designer-E, and their productivity is established. In the article "Design and Implementation of Cryptographic Element Multiplexer with Low Power Dissipation in Quantum Dot Cellular Automata," the authors S. Umira R. Qadri, Z. A. Bangi, M. Tariq Banday, and G. Mohiuddin Bhat [37] that Quantum Dot Cellular Automata is a novel innovation that enables the examiners to concentrate on unique advanced circuits. Nonetheless, it is necessary to approach these circuits so that an inventor might receive actual assistance. A multiplexer is one such important circuit in this area that enables secure message communication as a cryptographic component to save a clock cycle or to alter the channel partition track and has additionally been used to plan a variety of other beneficial circuits. In quantum spot cell automata, which is advantageous in information correspondence, this work proposes unique and effective designs of 2:1, 4:1, and 8:1 multiplexers with no hybrid. In terms of cell count, cell region, speed, dormancy, intricacy, and other factors, the three newly developed multiplexers have been compared to various most current designs, and the results show notable improvements. The introduced multiplexer structures are further implied to be entirely robust, greatly suitable for high temperature/recurrence, and can be used as a cryptographic component in secure message exchange by reenactment using QCA Creator and QCA Genius.

V. MOTIVATION

We could realize the main aspect to consider the different observation for standard implication to the secure nano-communication in the aspect of Quantum Dot Cellular Automata(QCA) in the field of nanotechnology. Thus the main important factor is thermodynamic effect for adjacent QCA cell are the biggest achievement through the implementation for security enhancement protocol in quantum inspired phenomenon.

➤ *Thermodynamic Considerations*

The QCA worldview depends on the actual cluster unwinding to its ground state to achieve the figuring. At nonzero temperature conditions of the framework might debase the result into a warm normal of right and erroneous out-comes. Since there are no power rails to get inside cells far from their thermo-dynamic balance state[29],[30] warm impacts will continuously be lethal to the plan at sufficiently high temperatures.

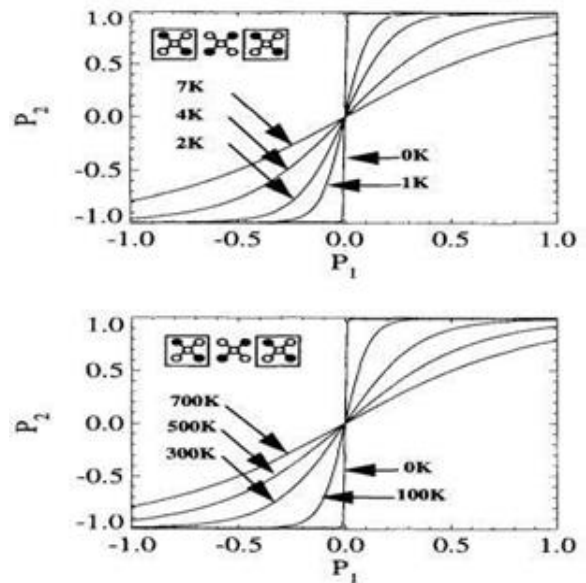


Fig 9 The cell response function for a cell driven on both sides at various temperatures. a) The response of the standard cell with inter-dot distance 20nm and relative dielectric constant 10. b) The response of a macromolecular cell with inter-dot Distance 2nm and relative Dielectric constant 1[25]

➤ *Thermodynamics of A Single QCA Cell*

Look at first as a "standard" QCA cell with the aspects and boundaries examined exhaustively in Ref.[26]. The focuses of the quantum spots in the cell are 20nm separated and the boundaries of the material are those of Ga As with a general dielectric consistent of 10. Process a marginally unique cell re-action bend than that in Figure 10 the cell polarization P_1 is prompted when the phone is driven by two adjoining cells with polarization P_2 . This reaction capability $P_1(P_2)$ is helpful on the grounds that it tends to be shown that a line of cells will spellbind with a worth of the polarization given by the proper place of rehashed cycles of this reaction bend.

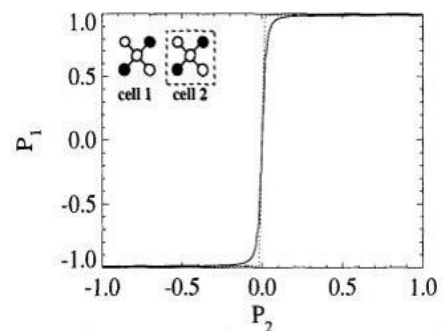


Fig. 10: The cell-cell response function. The polarization of the right cell is fixed and the induced polarization in the left cell is calculated by solving the two electron Schrodinger equation. The nonlinear nature of this response curve plays the role of gain in restoring signal levels from stage to stage [26]

➤ *Thermodynamics of A QCA Array Predicted with Realization of the Design*

Consider a planar QCA exhibit of N cells, each cell containing 5 quantum dots and 2 overabundance electrons of inverse twists. A planar exhibit of cells is displayed in Fig. 11. The all out Hamiltonian for the cluster is given by

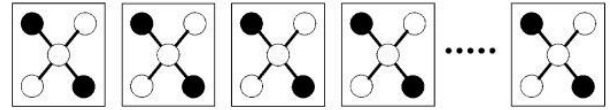


Fig 11 A QCA Array with Five Dots in Each Cell[33]

Here H_m is the Hamiltonian for the single disengaged cell, m and commu-nicated as in equation(1)

$$\hat{H} = \sum_{m=1} \hat{H}_m + \sum_{m < p} \hat{V}_{int}^{m,p} \tag{1}$$

$$\hat{H}_m = \sum_{i,\sigma} E_0 \hat{n}_{i,\sigma} + \sum_{i > j, \sigma} t_{ij} (\hat{a}_{i,\sigma}^+ \hat{a}_{j,\sigma} + \hat{a}_{j,\sigma}^+ \hat{a}_{i,\sigma}) + \sum_i E_Q \hat{n}_{i\uparrow} \hat{n}_{i\downarrow} + \sum_{i > j} \frac{e_i e_j}{4\pi\epsilon_0\epsilon_r |\vec{r}_i^m - \vec{r}_j^m|} \hat{n}_{i\uparrow} \hat{n}_{i\downarrow} \tag{2}$$

While $\hat{V}_{int}^{m,p}$ is the part of the Hamiltonian operator which depicts the electrostatic collaboration between the cells m and p:

$$\hat{V}_{int}^{m,p} = \sum_{i,j=1}^5 \sum_{k,q=1}^5 V(r_i^m, r_j^m, r_k^p, r_q^p) \hat{n}_{i\uparrow}^m \hat{n}_{i\downarrow}^m \hat{n}_{k\uparrow}^p \hat{n}_{q\downarrow}^p \tag{3}$$

Here, $V(r_i^m, r_j^m, r_k^p, r_q^p)$ is the electrostatic energy of collaboration be-tween two cells when electrons are limited in the given positions i, j, k and q. The first and second spiral vectors address electrons with turn "up" and "down" designs in a cell, separately. It would be ideal for it to be referenced here that every one of the terms in the aggregate Hamiltonian are traditional with the exception of the burrowing part,

$$\hat{T} = \sum_{cells} \sum_{i > j, \sigma} = \sum_{i > j, \sigma} t_{ij} (\hat{a}_{i,\sigma}^+ \hat{a}_{j,\sigma} + \hat{a}_{j,\sigma}^+ \hat{a}_{i,\sigma}) \tag{4}$$

Here and in the continuation, h_{cl} will be utilized for the traditional part. The premise in the Hilbert space of a cell of five destinations with two electrons of inverse twists is given by

$$|\Phi_{ij}\rangle = \begin{pmatrix} 0 \dots 1_i \dots 0 \\ 0 \dots 0 \ 1_j \ 0 \end{pmatrix}, \text{ Where } [i, j = 1, \dots, 5] \tag{5}$$

Here I and j are the site files in the cell. The first column is utilized for turn "up" state and the subsequent one is for turn "down", while the segments address the electron site in a cell. The state vector of the cell is

$$|\Psi\rangle = \sum_{i,j=1}^5 \Psi_{ij} \Phi_{ij} \tag{6}$$

The single-molecule density, ρ_q ; is determined utilizing the two-molecule state vector, $|\Psi\rangle$ from the assumption worth of the number administrator for site q:

$$\rho_q = \sum_{\sigma} \langle \Psi | \hat{n}_{q,\sigma} | \Psi \rangle = \sum_{\sigma} \sum_{i,j=1}^5 \sum_{k,q=1}^5 \Psi_{ij}^* \Psi_{km} \langle \Phi_{ij} | \hat{n}_{q,\sigma} | \Phi_{km} \rangle = \sum_{k=1}^5 (|\Psi_{kq}|^2 + |\Psi_{qk}|^2) \tag{7}$$

Think about a line of N QCA cells, the paired wire, driven from one end by a cell fixed to a polarization of +1. The ground state comprises of all cells with +1 polarization and it is non-degenerate. The ground state and the initial two energized states are displayed in Figure 11. In the main energized express, a few cells line up appropriately with the driver however at that point a "kink" happens and the ensuing cells all have the contrary polarization.

The kink is vigorously expensive in light of the fact that adjoining cells have inverse polarization. The energy of a kink is, to a decent estimation, free of wrinkle position and meant E_{kink} . The kink can be in any situation along the line bringing about a decadence of the principal energized province of $N-1 = N$. The second energized state is a two wrinkle state with energy $2E_{kink}$ and has a decline of generally N_2 . Summing up to higher energized states is direct[27].

As the quantity of cells builds the ground state stays one of a kind and the partition between ground state and first invigorated state remain E_{kink} . Nonetheless, the rising decline of the invigorated state implies it is increasingly more reasonable that As the quantity of cells expands the ground state stays extraordinary and the detachment between ground state and first energized state remain E_{kink} . Nonetheless, the rising decline of the energized state implies it is increasingly more reasonable that the framework at nonzero temperature 10 will be tracked down in an invigorated state – yielding a mix-up. This can be measured by considering the Helmholtz free energy of the framework $F = E - T_s$. The entropy of the n^* invigorated state is the framework at nonzero temperature.

$$S_n = K_B n \ln(N) \tag{3.1}$$

The difference in free energy between the zero-kink and n_{kink} state is then,

$$\Delta F_n = nE_{kink} [1 - \frac{K_B T}{E_{kink}} \ln(N)] \tag{3.2}$$

When this value ceases to be positive, the state with mistakes in the output cells becomes the thermodynamic equilibrium state. As long as this value is positive, the correct results appear at the output[28].

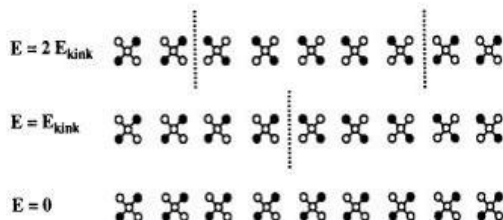


Fig. 12: Ground state and first two excited states of a line of cells. The left-most cell is assumed fixed[27]

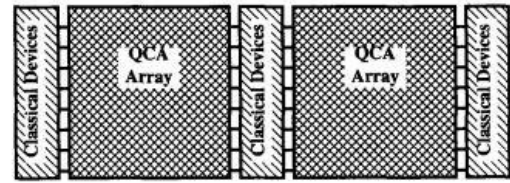


Fig. 13: Schematic of several QCA arrays with classical interface layers[28]

VI. SECURE NANOCOMMUNICATION USING QCA

Secure communication is very much important for data privacy. Now a days it is also implicated more authenticated way to consider for sharing some information in between sender and receiver. In this proposed technique is relevant the actual phenomenon for considering the same kind of assumption through channel coding in a nano communication network.

- *Cryptography*
Cryptography is an encoding (changing) strategy where message from clear structure to non-meaningful structure to give security[30] from an unauthorized access [14],[15].
- *QCA Encryption and QCA Decryption*
Encryption is a way of converting a regular instant message into an unrecognizable code, and decryption is the reverse cycle of changing the code into an instant message, as shown in Fig 9.[12]
- *QCA Plain Text and QCA Cipher Text*
Generic content is a message that can be received by the sender, recipients, and others with access to the content[29]. Then, using the appropriate scheme to construct the generic content, the subsequent message is called the ciphertext.

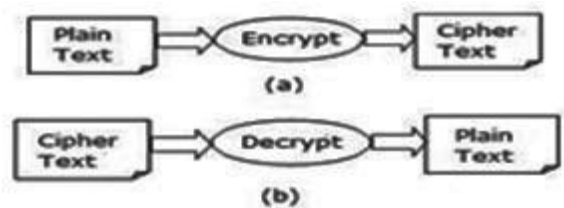


Fig 14 Encryption System and Decryption System

- *Stream Cipher and Block Cipher*
The plain text should be possible in symmetrical key cryptography in two basic ways – stream code as well as square code [14],[15]. Each byte is then scratched with the key in the current figure and plain content is encrypted on block figure in a square of bytes, all with the key shown in Figure 15.

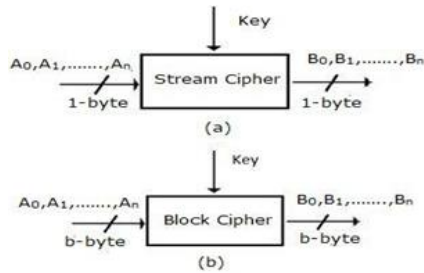


Fig 15 QCA Stream Cipher and QCA Block Cipher

➤ *QCA Encryption and Decryption in Stream Ciphers*

Suppose plain text, ciphertext along with stream key comprises singular pieces, such as $(A_i, B_i, K_i \in \{0, 1\})$. At that point structure [15] the meaning of encryption as well as decoding capacity may be composed as

Encryption:

$$B_i = EK_i(A_i) \equiv A_i + K_i \pmod{2} \tag{IV}$$

Unscrambling:

$$A_i = DK_i(B_i) \equiv A_i + K_i \pmod{2} \tag{V}$$

The relating outline is appeared in Figure 16.

In reality encryption as well as decoding capacity are coherently similar [15] as demonstrated below

$$DK_i(B_i) \equiv A_i + K_i \pmod{2} \equiv (A_i + K_i \pmod{2}) + K_i \pmod{2} \text{ [From articulation 1]} \equiv A_i + K_i \pmod{2} + K_i \pmod{2} \equiv A_i + 2K_i \pmod{2} \equiv A_i + 0 \pmod{2} \equiv A_i \pmod{2} \text{ Q.E.D}$$

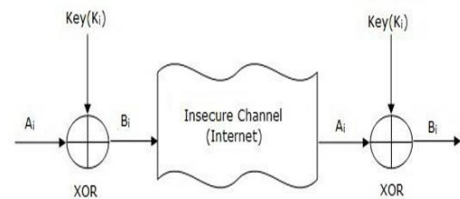


Fig. 16: Encryption and Decryption using Stream Ciphers

Now, the articulation estimation $(2K_i \pmod{2})$ is consistently zero as $(0 \pmod{2}) \equiv 2$. Now, If $K_i = 0$ then $2K_i = 2 \cdot 0 \equiv (0 \pmod{2})$.

Also, on the off chance that

$$K_i = 1, 2K_i = 2 \cdot 1 = 2 \equiv (0 \pmod{2})$$

Throughout encryption as well as decoding cycle to create figure text and plain content individually, XOR coherent activity is utilized as in light of the fact that the activity $B_i = EK_i(A_i) \equiv A_i + K_i \pmod{2}$ generate yield, which is identical to XOR yield entryway activity as demonstrated in table 2 and 3.

Table 2 Encryption Operation Truth Table

A_i	K_i	$B_i \equiv A_i + K_i \pmod{2}$
0	0	0
0	1	1
1	0	1
1	1	0

Table 3 Truth table of xor operation

A_i	K_i	B_i
0	0	0
0	1	1
1	0	1
1	1	0

The first single material is without question created from plain text as seen in Figure 12, since XOR operation is reversible.

The expression 3 & 4 were rewritten from the XOR-gate truth table as in Table 2.

$$B_i = EK_i(A_i) = A_i \oplus K_i = A_i K_i + A_i \bar{K}_i \tag{VI}$$

$$A_i = DK_i(B_i) = B_i \oplus K_i = B_i K_i + B_i \bar{K}_i \tag{VII}$$

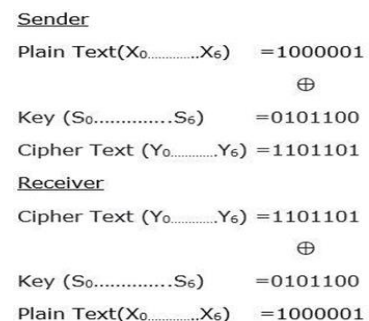


Fig 17 Example of Encryption and Decryption

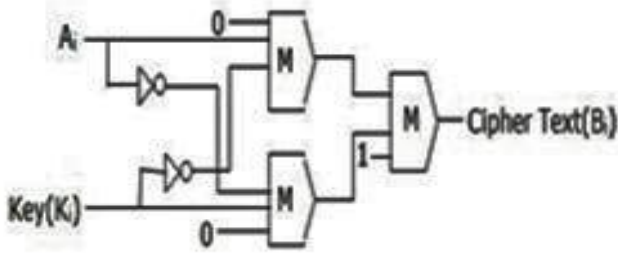


Fig 18 Cipher Text Generation Schematic in QCA

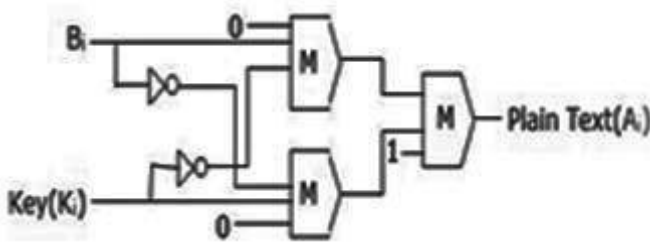


Fig 19 Plain Text Generation Schematic in QCA

The outline shown in Figure 13 and Figure 14. The relevant consideration in QCA and below is an expansion of the related majority gate expression:

$$B_i = F(F(A_i, K_i, 0), F(A_i, K_i, 0), 1) \quad \text{(VIII)}$$

$$A_i = F(F(B_i, K_i, 0), F(B_i, K_i, 0), 1) \quad \text{(IX)}$$

We are assuming for symmetric key cryptography, the above depiction relies the several plain to one cipher text and in case of decoder the several cipher text to one plain text for assuming as a mux and demux is encryption and decryption symmetric sequence cryptography.

Nano communication is secure for different aspect, so we need to recom-mend Nano network with channel-encrypted pseudo-binary sequence generator for Crypto network in model prediction. It is generally used to in advanced correspondence frameworks to shield the computerized data from commotion and obstruction and diminish the quantity of bit errors & is generally refined by specifically redundant bits into the sent data stream.

VII. PSEUDORANDON BINARY SEQUENCE(PRBS) GENERATOR

We are proposing 1 bit PRBS generator to implicate this finding & application for insecure channel to secure one channel coding. Here the following figure illustrates Pseudo Random Binary Sequence generator circuit.It has applied the concept in case of QCA nanocommunication for cryptographic application which is utilized as a key that automatically changes for every kind of simu-lation & also increases the possibility to protect against unauthorised access from encryption & decryption in this secure nanocommunication network.

The PRBS depicts that we have to realize for fixed sequence 5 “zeros” & 3 “ones”(i.e 8 bit as 01001100) but position will change as of pseudorandom sequence for PRBS

generator in the output waveform and have a major role in QCA nanocommunication network for channel coding application.

VIII. REDUCE BIT ERROR RATE IN CHANNEL CODING APPLICATION

Reducing transmission capacity is one way that can be used to lower the bit error rate. Lower levels of commotion will be attained, and as a result, the ratio of sign to clamour will increase. Once more, this reduces the amount of information that can be processed. As we must fundamentally express our data as an 8-digit sequence, the bit error rate in this phenomenon is reduced to 10^8 bits per second. In order to improve signal quality and lower the bit error rate, channel coding is performed (BER). A channel coding method is used to fix transmission problems that happen on the specific channel. Channel jitter, impedance, torsion, problems with bit timing, restrictions, remote multipath interference, and other factors can all have an impact on the receiver side BER in the appropriate setup. By choosing a strong signal strength (as long as it doesn’t lead to crosstalk and more partial mistakes), selecting a slow and strong tuning plane or a stream encoding plane, and using channel coding management techniques such repeat forward error correction codes, the BER can be increased. The number of erroneously recognised portions prior to error correction, divided by the number of full motion bits, is known as the transmit BER (counting of repeated error codes). The number of decoded bits that still include mistakes after the error modifications, divided by the entire number of decoded bits, is known as the BER data, which is essentially comparable to the integral error probability (the payload). The transmission BER typically exceeds the data BER. The forward error correction (FEC) code’s strength has an impact on the BER data.

IX. SCHRODINGER EQUATION FOR QUANTUM ENHANCEMENT SECURITY LEVEL TO OPTIMIZED QUANTIZED STATES

Burrowing electrons have double wave molecule property. Every electron molecule, while traveling through the passage, carries on the collectively of waves as pro-posed by deBroglies speculation on related waves [12],[13]. As indicated by this theory this gathering of waves is the only superposition of a few monochro-matic waves with identical plentifulness and stage however imperceptibly with varied frequency [14],[15]. Let the superposition condition of an electron bur-rowing between the spots the a way be $\psi(a)$. Fourier change communicates the superposition

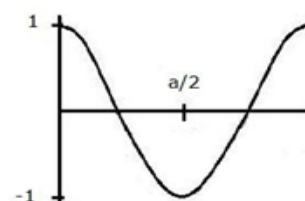


Fig 20 QCA cell in 2D representation [20]

an electron's state (a),

$$\psi(a) = \frac{1}{2\pi} \int_{-\infty}^{\infty} \phi(s) e^{i(sa)} ds \tag{10}$$

Where the adequacy of the superposition wave is represented by $\psi(k)$. $k = 2\pi/\lambda$ is the wave spread speed, the wavelength is denoted by λ and $i = \sqrt{-1}$ the trademark bend of an electron wave is illustrated by Figure 21 while moving through channels [19]. At whatever point electron is confined, it is situating at $x = 0$ and $e^{i(kx)} = 1$ achieved this value. It implies electron influxes with varied frequencies meddle valuably and no motions are announced. Henceforth $\psi(x)$ achieves top at $x = 0$ with varying upsides of x , the segments of $e^{i(kx)}$ are inserted in Equation 10. In this way bringing about motions and the worth of $\psi(x)$ is acquired. At $x/2$, $e^{i(kx)}$ accomplishes least worth and trademark bend

As expressed before, a clock signal is the energy provider to the electrons for changing their state. We accept that between spot channels are encountering infinite $V(a)$ potential energy in the positive a direction. At that point time, autonomous Schrodinger wave condition is,

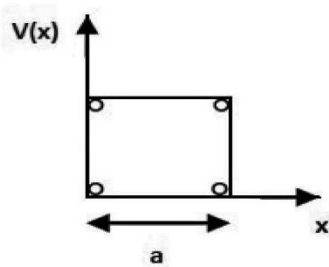


Fig 21 Characteristic Curve [20]

$$\frac{p^2 \psi(a)}{da^2} + \frac{2m}{\hbar^2} (En - V(a)) \psi(a) = 0 \tag{11}$$

where electron mass is denoted by m , decreased plank constant by \hbar [15],[24], In finite arrangement of discrete energy levels is expressed by E_n relating to all conceivable non-negative basic upsides of n . whereas the quan-tum number is given by n . Condition 12 can be diminished to

$$E_n = \frac{n^2 \pi^2 \hbar^2}{2mp^2} + V(a) \tag{12}$$

where p is the distance between two sub-atomic cells [19]. Whenever voltage is given to the atom as V volt with C junction capacitance at that point, articulation will be produced as [16],

$$\frac{n^2 \pi^2 \hbar^2}{2mp^2} + V(a) = \frac{1}{2} CV^2 \tag{13}$$

This articulation will help to compute the working RMS voltage of the framework.

To compare two quantum numbers n_1 and n_2 , we need two discrete states i.e. E_{n1} and E_{n2} . The electron may travel starting with one energy state then onto the next if the whole or contrast of quantum no. is an even number[19]. To move from this condition to the ground, we must discover the n th quantum number, the energy is transmitted by a cell between 3.85×10^{-3} eV to 10^{-4} eV . This change is communicated as,

$$\Delta E = E_n - E_1 = \frac{\pi^2 \hbar^2}{mb^2} (n^2 - 1) \tag{14}$$

Producing framework needs to emanate energy in the reach between 3.85×10^{-3} eV to 10^{-4} eV . Considering most reduced energy esteem i.e., 3.85×10^{-3} eV to be equivalent to ΔE in Equation 15, the distance between one cell to another one (p) and quantum no. (n) is given as

$$n^2 - 1 = 16.24 \times 10^{-41} p^2 \tag{15}$$

Now, the most elevated energy radiation that is 10^{-4} eV is being taken into account and comparing it to ΔE_n in Equation 16, the distance between two sub-atomic cell (p) and quantum no. (n) is given as

$$n^2 - 1 = 2.59 \times 10^{-42} p^2 \tag{16}$$

A cautious investigation of Figure 24 outcomes that at $2 V_{rms}$ working voltage as well as a temperature of 1000 K the phones accomplish a component of 10 nm believing the expected energy of an electron to be 4.2×10^{-20} Joules and the value of C will be 200 atto-farad. If atomic cell measurement is viewed as 10 nm, for the most minimal degree of radiation, Equation 15 creates the worth of n to be 290. On the off chance that we apply a similar technique in Equation 16 for the most elevated restriction of radiation, the value of n will be 298, with $1300^\circ C$ updated temperature value at a voltage of $2.81 V_{rms}$ for a solitary atomic cell, Equation 16 should be written as,

$$v_2 = \frac{\pi \hbar}{2mp^2} (n^2 - 1) \tag{17}$$

where v_2 is radiation frequency.

Equation 16 produces the corollary that $v_2 = 1.015 \times 10^{15}$ Hz has a value of $n=298$ and $d=10$ nm and $v_2 = 9.612 \times 10^{14}$ Hz with $n= 290$ and $d = 10$ nm ranges from 1×10^{15} Hz to 10^{15} Hz, the repeat range of the existing frame. The above calculations are for a subatomic cell. The intensity of the radiant energy for N subatomic cells arranged in a course is recorded in the range of $3.8510^{-3} \times N$ to 10^{-4} times N . We have also shown the variation of potential energy in different states of quantum level. It is illustrated in Figure 21 and Figure 22 calculated from the open source[20].

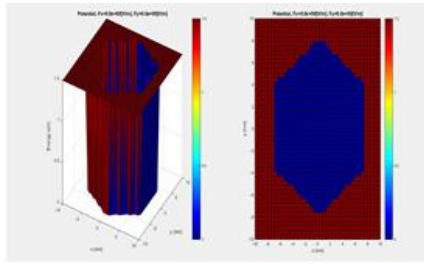


Fig 22 Schrodinger 2D wave equation for 1st approach(n=3) of Quantum number

Here we have computed the different condition for "n" value approaches in a Tabular formation. It also has analysed in Table 4.

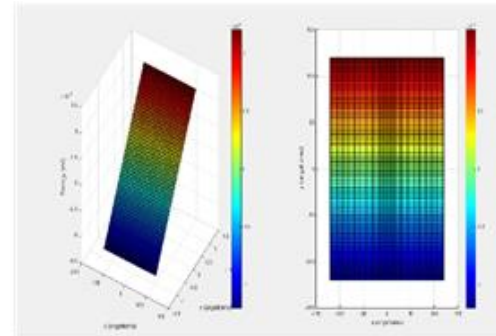


Fig 23 Schrodinger 2D wave equation for 2nd approach(n=4) of Quantum number

Table 4 Comparative study of different n value approaches in the state of Quantum level

Theoretical Assumption	Expression	Energy	Value of Quantum number
Quantum Enhancement Security for Quantum number & cell dimension[Existing] [20]	$n^2 - 1 = 13.29 \times 10^{-21} p^2$	$5 \times 10^{-3} \text{ ev to } 10^{-4} \text{ ev}$	116
Quantum Enhancement Security for Quantum number & molecular cell dimension[Existing][20]	$n^2 - 1 = 2.66 \times 10^{-22} p^2$	10^{-4} ev	162
Quantum Enhancement Security for Quantum number & cell dimension[Proposed]	$n^2 - 1 = 16.24 \times 10^{-41} p^2$	$3.85 \times 10^{-3} \text{ ev to } 10^{-4} \text{ ev}$	290
Quantum Enhancement Security for Quantum number & molecular cell dimension[Proposed]	$n^2 - 1 = 2.59 \times 10^{-42} p^2$	10^{-4} ev	298

X. RESULTS AND DISCUSSIONS

The circuit was executed and imitated using the Bistable QCA Designer 2.0.3 game engine [10], yield came after the second control span as shown in Figure 15 and confirmed using the pinboard. sole reason. Figure 15 shows the end of the encoder when $K_i = 0, A_i = 1$ then $A_i = 0$ and $B_i = 1, K_i = 1$ then $B_i = 1$, etc as shown by the green circle. At the end of decoder when $K_i = 0, B_i = 1$ then $A_i = 1$ and $K_i = 1, B_i = 1$, then $A_i = 0$, etc as indicated by the blue mark. Attached limits used to estimate determinable: impact radius 65.00 nm, Clock high 9.810^{22} J , 1,000 maximum iterations, 12,800 times test, 12,900 Relative License, 5 nm Spot Distance, 20 nm Cell Size, and 20 nm Cell Width. 2.0000 is set to the clock crest factor, 11.50000 nm is set to layer separation, 0.001000 convergence tolerance and 3.810^{23} J lower clock.

XI. CONCLUSIONS

Due to the creation of side-channel attacks, crypto utility can be exploited to the extent of brute force and electromagnetic forensic attacks. With that, since QCA has extremely low force usage and extremely fast time rates, the proposed circuit can be a guiding principle for creating a secure QCA encryption module instead of one. normal size. Encryption as well as decryption is done on a 7 bit message using a 7 bit key, but it can very well be done on any length of message bit as well as key material using a offer. The

circuit now requires only 3 MVs, 42 cells, 3 clock regions, 2 inverters, as well as 36,000 nm² regions for the decoder and encoder. For such a view, we have shown more secure encryption in this cryptographic approach in QCA. This indicates and improves more secure authentication through channel encryption in nanocommunication networks with Pseudo-Random Binary Sequence (PRBS). Future performance of cryptographic calculations for a secure nano-matching framework based on QCA can be performed using this proposed circuit.

REFERENCES

- [1]. M. Niemer, P. Kogge, Problems in designing with qcas: Layout = timing, Int. J.Circuit Theory Appl 29 (2001) 49–62.
- [2]. S. Umira, R. Qadri, Z. Bangi, M. Banday, G. Bhat, A novel cryptographic design in quantum dot cellular automata (2018) 1–6.
- [3]. C. Lent, P. Tougaw, A device architecture for computing with quantum dots, Vol. 85, 1997, pp. 541–557.
- [4]. B. Debnath, J. Das, D. De, S. Mondal, A. Aumadian, M. Salimi, M. Ferrara, Security analysis with novel image masking based quantum-dot cellular automata information security model, IEEE 8 (2020) 117159–117172.
- [5]. K. Navi, S. Sayedsalehi, R. Farazkish, M. R. Azghadi, Five-input majority gate, a new device for quantum-

- dot cellular automata, *Comput. Theor. Nanoscience* 7 (2010) 1546–1553.
- [6]. P. Singh, A. Majumder, B. Chowdhury, R. Singh, N. Mishra, A novel realization of reversible lfsr for its application in cryptography (2015) 601–606.
- [7]. M. Amiri, M. Mahdavi, S. Chaki, Qca implementation of a5/1 stream cipher (2009) 48–51.
- [8]. V. Vankamamidi, M. Ottavi, F. Lombardi, A serial memory by quantum dot cellular automata (qca), *IEEE Trans. Computer* 57 (2008) 606–618.
- [9]. W. Liu, S. Srivastava, L. Lu, M. O’Neill, E. Swartzlander, Power analysis attack of qca circuits: a case study of the serpent cipher (2013) 2075–2078.
- [10]. A. Cilaro, Exploring the potential of threshold logic for cryptography related operations, *IEEE Transactions on Computer* 60 (2011) 452–462.
- [11]. W. Liu, S. Srivastava, L. Lu, M. O’Neill, E. Swartzlander, Are qca cryptographic circuits resistant to power analysis attack?, *IEEE Transaction on Nanotechnology* 11 (2012) 1239–1251.
- [12]. S. Heikalabad, A. Navin, M. Hosseinzadeh, Midpoint memory: A special memory structure for data-oriented models implementation, *Journal of Circuits, Systems and Computers* 24 (2015) 1550063(1)–1550063(14).
- [13]. K. Datta, D. Mukhopadhyay, P. Dutta, Comprehensive study on the performance comparison of logically reversible and irreversible parity generator and checker designs using two-dimensional two-dot one electron qca, *Microsystem Technologies* (2017) 1–9 doi:10.1007/s00542-017-3445-2.
- [14]. M. Ghosh, D. Mukhopadhyay, P. Dutta, A novel parallel memory design using 2 dot 1 electron qca (2015) 485–490.
- [15]. K. Chakrabarti, Realization of original quantum entanglement state from mixing of four entangled quantum states 863. doi:https://doi.org/10.1007/978-3-030-34152-712.
- [16]. D. Mukhopadhyay, P. Dutta, A study on energy optimized 4 dot 2 electron two dimensional quantum dot cellular automata logical reversible flip-flops, *Microelectronics Journal* 46 (2015) 519–530.
- [17]. M. Ghosh, D. Mukhopadhyay, P. Dutta, A 2d 2 dot 1 electron quantum dot cellular automata based logically reversible 2:1 multiplexer (2015) 1–6.
- [18]. D. Mukhopadhyay, P. Dutta, Quantum dot cellular automata based novel unit reversible multiplexer, *Advance Science Letters* 5 (2012) 1–6.
- [19]. K. Datta, D. Mukhopadhyay, P. Dutta, Comprehensive design and analysis of gray code counters using 2-dimensional 2-dot 1-electron qca, *Microsystem Technologies* (2018) 1–19 doi:0.1007/s00542-018-3818-1.
- [20]. <https://github.com/LaurentNevou/Qschrodinger2Dpemo>.
- [21]. G. Bernstein, A. Imre, V. Metlushko, A. Orlov, L. Zhou, L. Ji, G. Csaba, W. Porod, Magnetic qca systems, *Microelectron. J* 36 (2005) 619–624.
- [22]. M. Amiri, M. Mahdavi, R. Atani, S. Chaki, Qca implementation of serpent block cipher (2009) 16–19.
- [23]. S. Hashemi, K. Navi, New robust qca d flip flop and memory structures, *Microelectronics* 43 (2012) 929–940.
- [24]. K. Chakrabarti, Is there any spooky action at a distance? 170. doi:https://doi.org/10.1007/978-981-33-4084-865.
- [25]. P. D. Tougaw, C. S. Lent, and W. Porod, *J. Appl. Phys.* 74, 3558 (1993).
- [26]. P. D. Tougaw, C. S. Lent, *J. Appl. Phys.* 75, 1818 (1994).
- [27]. M. Field, C.G. Smith, M. Pepper, J.E.F. Frost, G.A.C. Jones, and D.G. Hasko, *Phys. Rev. Lett.* 70, 13 11 (1993).
- [28]. P. Lafarge, H. Pothier, E.R. Williams, D. Esteve, C. Urbina, and M.H. Devoret, *Z. Phys. B* 85, 327 (1991); D. Esteve, in *Single Charge Tunneling*, H. Grabert and M.H. Devoret, eds., (Plenum, New York, 1992) Chap. 3.
- [29]. Jadav Chandra Das and Debashis De, Computational fidelity in reversible quantum-dot cellular automata channel routing under thermal randomness, *Nano Communication Networks*, Volume 18, PP 17-26, 2018
- [30]. Jadav Chandra Das and Debashis De, Circuit switching with Quantum-Dot Cellular Automata, *Nano Communication Networks*, Volume 14, PP 16-28, 2017
- [31]. Ross Anderson and Robert Brady, Why quantum computing is hard - and quantum cryptography is not provably secure, *Quantum Physics (quant-ph); Cryptography and Security (cs.CR); Mathematical Physics (math-ph)* arXiv:1301.7351v1
- [32]. Debnath, B., Das, J.C., De, D.: Cryptographic models of nanocommunication network using quantum dot cellular automata: a survey. *IET Quant. Comm.* 2(3), 98–121 (2021). <https://doi.org/10.1049/qtc.2.12013>
- [33]. Mohammad Amin Amiri, Sattar Mirzakuchaki and Mojdeh Mahdavi, Cryptography in Quantum Cellular Automata, PP 285-296, DOI:10.5772/15967
- [34]. M. Amutha and K.R. Kavitha, Hardware Security based Quantum Dot Cellular Automata Circuit Design – Review and Outlook, ISSN:1583-6258, Vol. 25, Issue 5, 2021, Pages. 1934 - 1939
- [35]. Mansi Rana and Ajay Dagar, DESIGN AND ANALYSIS OF QCA CRYPTOGRAPHIC CIRCUITS, ISSN (Online): 2347 - 4718, Volume 5, Issue 8, PP 3509-3513, April-2018
- [36]. Hyun-Il Kim and Jun-Cheol Jeon, Quantum LFSR Structure for Random Number Generation Using QCA Multilayered Shift Register for Cryptographic Purposes, MDPI, *Sensors* 2022, 22, 3541. <https://doi.org/10.3390/s22093541>, PP 1-19, 6th May, 2022.
- [37]. S. Umira R. Qadri, Z. A. Bangi, M. Tariq Banday and G. Mohiuddin Bhat, Design and Implementation of Cryptographic Element Multiplexer with Low Power Dissipation in Quantum Dot Cellular Automata, *Nanomaterials and Energy* 2019, 8:1-13, doi: 10.1680/jnaen.18.00013.